# Specular electron scattering at single-crystal Cu(001) surfaces

J. S. Chawla and D. Gall[a)]
*Department of Materials Science and Engineering, Rensselaer Polytechnic Institute, New York 12180, USA*

(Received 22 April 2009; accepted 2 June 2009; published online 22 June 2009)

Epitaxial copper layers, 20 nm to 1.5-$\mu$m-thick, were grown on MgO(001) by ultrahigh vacuum magnetron sputter deposition at 80 °C. *In situ* electrical resistivity measurements indicate partial specular scattering at the Cu vacuum interface with a Fuchs–Sondheimer scattering parameter $p=0.6\pm0.1$. *In situ* deposition of 0.3 to 7.0-nm-thick Ta cap layers on the Cu surfaces leads to a resistivity increase, which is independent of the Ta thickness and is associated with a transition to completely diffuse surface scattering with $p=0.0\pm0.1$. The diffuse scattering is attributed to a "rough" electron potential at the Cu–Ta interface as well as to scattering into localized interface and surface states. © *2009 American Institute of Physics*. [DOI: 10.1063/1.3157271]

Electron scattering at Cu surfaces causes an increase in the resistivity $\rho$ of interconnecting lines in integrated circuits as the linewidth $d$ decreases to approach the mean free path $\lambda$ for electron–phonon collisions. This so-called "size effect" represents a major challenge to Moore's law for the continued down scaling of feature sizes[1,2] and has been quantified experimentally by various researchers for both thin films[3,4] and wires.[5–7] Other contributions to the size effect are scattering at grain boundaries, which typically increase in density with decreasing $d$, as well as surface roughness, which effectively reduces the cross-sectional area.[3,8–10] Due to these convoluted effects, a detailed quantitative understanding of electron scattering at Cu surfaces is still lacking.

Electron surface scattering events are classically described as either specular or diffuse and are quantified by the phenomenological scattering parameter $p$.[11] *Specular* scattering ($p=1$) refers to an elastic scattering event where the electron momentum perpendicular to the surface is reversed while the parallel component is conserved causing no effect on the resistivity. In contrast, *diffuse* scattering ($p=0$) results in a complete randomization of the electron momentum and a corresponding increase in the resistivity. Most studies on electron scattering at Cu surfaces report completely diffuse ($p=0$) scattering[3,8,12] while some results indicate positive $p$ values.[13–15] We attribute the discrepancy between the different researchers to the challenge in correctly accounting for grain boundary scattering and, to a lesser degree, variations in surface morphology. Our previous *ex situ* experiments also show completely diffuse surface scattering[4] but we predict specular scattering for atomically smooth oxygen-free Cu surfaces using *ab initio* calculations.[16] We have demonstrated single crystal Cu layers with 0.35 to 0.60-nm-wide atomically smooth terraces and root-mean-square (rms) surface roughness values between 0.4 and 1.8 nm.[4] Recent simulations predict that specular scattering should be achievable for rms roughness below 0.7 nm.[17] From these results, together with the fact that specular scattering has been observed by various researchers for Au surfaces,[18–20] we conclude that the primary reason for the reported completely diffuse scattering on Cu surfaces is due to rapid submonolayer oxidation in air.

In this letter, we circumvent all the above challenges in quantifying electron scattering on Cu surfaces by (i) using epitaxial single crystal layers to suppress grain boundary scattering, (ii) measuring resistivity *in situ* or in liquid $N_2$ to suppress surface oxidation, and (iii) limiting the rms surface roughness to <1.8 nm to render the geometric effect of surface roughness negligible. In addition, we deposit Ta cap layers *in situ* onto Cu films and measure the change in resistivity and, in turn, the specularity $p$. These measurements on the same Cu layer (with and without Ta) have the advantage that sample-to-sample thickness variations, which cause large uncertainties in the determination of $p$, are absent. They demonstrate that the addition of a few monolayers of Ta on Cu surfaces with initially partially specular scattering ($p=0.6\pm0.1$) results in Cu–Ta interfaces with completely diffuse scattering ($p=0.0\pm0.1$).

All layers were grown in a three-chamber ultrahigh vacuum dc magnetron sputtering system with a base pressure $<10^{-9}$ Torr. The polished MgO(001) substrates were cleaned with successive rinses in ultrasonic baths of trichloroethylene, acetone, isopropyl alcohol, and de-ionized water and thermally degassed at 800 °C in vacuum. The 5-cm-diameter Cu (99.999%) target was facing the substrate at 12 cm distance and deposition was performed in $2.5\pm0.2$ mTorr Ar (99.999 %) at 80 °C and at a constant power of 150 W, yielding a deposition rate of 1.3 nm/s. After deposition, the layers were transported without breaking vacuum to the analysis chamber for *in situ* resistivity measurements with a linear four point probe operated at 1–100 mA. The samples were allowed to self-cool to room temperature and thermal equilibrium was considered to be reached when the measured resistivity asymptotically approached a constant value that varied less than 0.1% per 1 h. Some samples were transferred back to the deposition chamber for Ta deposition followed again by *in situ* resistivity measurements. The measured resistivity was independent of the Ar pressure during Ta deposition, 2.5 to 20 mTorr, suggesting that residual defect formation due to backscattered Ar neutrals during Ta deposition is negligible. Cu layers without Ta cap were removed from the vacuum system by transfer to a load lock that was vented with dry $N_2$. The samples were dropped into liquid $N_2$ within 2 s after removal from the vacuum system to minimize surface oxidation followed by *ex situ* four point probe measurements in liquid $N_2$. The layer thicknesses were determined from the temperature dependence in the resistivity and were verified using Rutherford backscattering. Layer roughness was quantified by *in situ*

[a)]Electronic mail:galld@rpi.edu.

 © 2009 American Institute of Physics

Downloaded 23 Jul 2009 to 128.113.37.139. Redistribution subject to AIP license or copyright; see http://apl.aip.org/apl/copyright.jsp

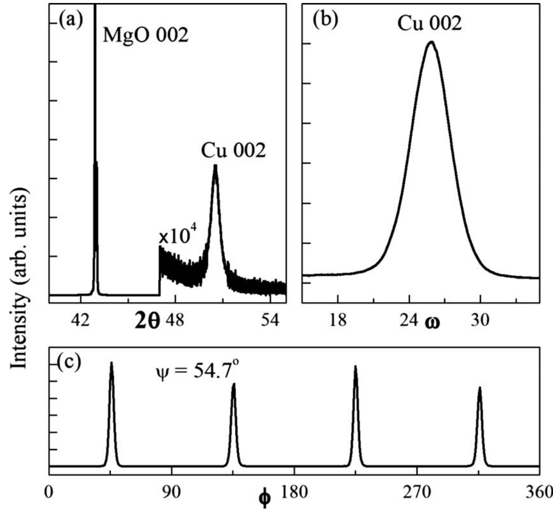


FIG. 1. (a) XRD $\omega$-$2\theta$ scan, (b) $\omega$ rocking curve from the Cu 002 reflection, and (c) Cu-111 $\phi$ scan at a tilt angle $\psi$=54.7°, from a 40-nm-thick Cu layer on MgO(001).

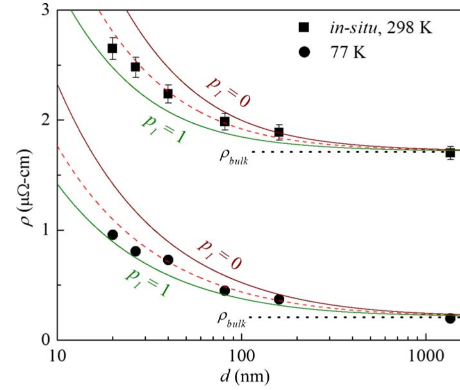


FIG. 2. (Color online) Resistivity $\rho$ of epitaxial Cu(001) layers vs layer thickness $d$ at 298 and 77 K. The solid lines represent the expected $\rho$ values from Eq. (3) for $p_1$=0, 0.5, and 1 at 298 and 77 K, as indicated.

scanning tunneling microscopy as described elsewhere[4,21] and was <1.8 nm for all Cu surfaces.

The resistivity measurements are discussed within the theoretical framework by Fuchs and Sondheimer (FS),[11,22] who derived the following expression that integrates over all classical electron paths to predict the effect of surface scattering on the resistivity $\rho$ for a thin film of thickness $d$

$$\rho = \rho_{\text{bulk}}\left[1 - \frac{3}{2\kappa}(1-p)\int_1^{\infty}\left(\frac{1}{t^3} - \frac{1}{t^5}\right)\frac{1 - e^{-\kappa t}}{1 - pe^{-\kappa t}}dt\right]^{-1}, \quad (1)$$

where $\kappa = d/\lambda$. $\lambda$ is calculated using the Fermi free electron model and the experimental bulk resistivity $\rho_{\text{bulk}}$. The values for room-temperature (298 K) Cu are $\rho_{\text{bulk}} = 1.712\ \mu\Omega$ cm (Ref. 23) and $\lambda = 39$ nm. FS also derived a more convenient approximation for Eq. (1)

$$\rho = \rho_{\text{bulk}}\left[1 + \frac{3}{8\kappa}(1-p)\right] \quad (2)$$

which is accurate to within 2% for $\kappa \geq 0.5$ at $p = 0.5$.[24] Eqs. (1) and (2) assume that scattering at the top or the bottom surfaces exhibit the same specularity. However, our layers, as well as typical metal interconnect structures, exhibit distinctly different top and bottom surfaces with correspondingly different specularity parameters $p_1$ and $p_2$, respectively. We use a similar approach as FS to derive

$$\rho = \rho_{\text{bulk}}\left[1 - \frac{3}{4\kappa}\int_1^{\infty}\left(\frac{1}{t^3} - \frac{1}{t^5}\right)\frac{2(1 - p_1p_2e^{-\kappa t})(1 - e^{-\kappa t}) - (p_1 + p_2)(1 - e^{-\kappa t})^2}{1 - p_1p_2e^{-2\kappa t}}dt\right]^{-1} \quad (3)$$

and the approximate form

$$\rho = \rho_{\text{bulk}}\left[1 + \frac{3}{8\kappa}\left(1 - \frac{p_1 + p_2}{2}\right)\right], \quad (4)$$

which is accurate to within 6 % for $\kappa \geq 0.5$ at $p_{\text{average}} = (p_1 + p_2)/2 = 0.5$.

Figure 1 shows exemplary x-ray diffraction (XRD) results from a 40-nm-thick Cu/MgO(001) layer obtained using a Bruker D8 system with a Cu $K_\alpha$ source and a Goebel mirror that provides a parallel incident beam. The only observable peaks in a $\omega$-$2\theta$ scan from 40 to 90° $2\theta$ are the MgO 002 and the Cu 002 reflections at 42.91° and 50.50°, shown in Fig. 1(a), corresponding to measured lattice constants of $a_{\text{MgO}} = 0.4211$ nm and $a_{\text{Cu}} = 0.3612$ nm, respectively. The latter value is 0.08 % below the reported lattice constant for bulk Cu, 0.3615 nm, indicating a slight biaxial tensile stress causing an in-plane strain of $\varepsilon_2 = 0.1\%$ determined using a Poisson ratio $\upsilon_{\text{Cu}} = 0.33$. The tensile stress is attributed to the misfit of Cu on MgO, $(a_{\text{MgO}} - a_{\text{Cu}})/a_{\text{MgO}} = 14.22\%$. The Cu 002 peak in Fig. 1(a) is relatively broad, with a full-width-at-half-maximum (FWHM) of 0.73°, corresponding to a x-ray coherence length of 14 nm, which is below the layer thickness of 40 nm, indicating residual strain variations and/or crystalline defects within the Cu layer. Figure 1(b) shows the corresponding $\omega$ rocking curve of the Cu 002 peak at a constant $2\theta = 50.50°$. The FWHM of 3.3° indicates strong alignment of the Cu along 001 but is large enough that the Cu may be slightly tilted to relieve misfit strain as previously reported.[25] XRD pole figure measurements with constant $2\theta$ values corresponding to Cu 002 and Cu 111 reflections at 50.42° and 43.32°, respectively, show only a single peak for Cu 002 at the origin (not shown) and four peaks at a tilt angle $\psi = 54.7°$ for Cu 111, presented in Fig. 1(c) as $\phi$ scan. The peaks are at fourfold symmetric polar angles $\phi$ = 45°, 135°, 225°, and 315° and exhibit an average FWHM of 3.5°. The pole figure analyses confirm a cube-on-cube epitaxial relationship of the Cu layer with the MgO substrate: Cu(001)‖MgO(001) and Cu[100]‖MgO[100], in agreement with previous reports, which also state that the large misfit strain is relieved by 7×7 Cu unit cells fitting on 6×6 MgO cells.[25]

Figure 2 is a plot of the resistivity $\rho$ of Cu layers with bare Cu(001) surfaces versus layer thickness $d$, measured both in vacuum at 298 K and in liquid nitrogen at 77 K. The thickest layer with $d = 1.40 \pm 0.03\ \mu$m exhibits $\rho$ values of $1.70 \pm 0.06$ and $0.196 \pm 0.004\ \mu\Omega$ cm at 298 and 77 K, respectively. These values are close to the expected Cu bulk resistivity at the respective temperatures, $\rho_{\text{bulk}}^{298\text{ K}} = 1.712\ \mu\Omega$ cm and $\rho_{\text{bulk}}^{77\text{ K}} = 0.213\ \mu\Omega$ cm. As $d$ decreases, the resistivity increases up to $2.65 \pm 0.09$ and $0.96 \pm 0.03\ \mu\Omega$ cm for $d = 20.0 \pm 0.4$ nm at 298 and 77 K, respectively. This increase is attributed to electron scattering

Downloaded 23 Jul 2009 to 128.113.37.139. Redistribution subject to AIP license or copyright; see http://apl.aip.org/apl/copyright.jsp

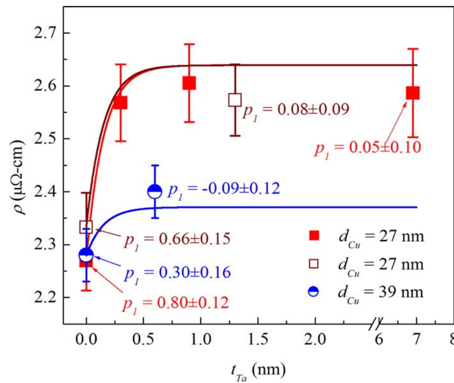


FIG. 3. (Color online) Measured Cu resistivity $\rho$ vs the thickness $t_{Ta}$ of a Ta cap layer deposited *in situ* on a Cu(001) layer. The solid lines are the expected values when assuming an exponential decay in specularity.

at the top and bottom surfaces, which correspond to bare Cu(001) and to the Cu–MgO interface. The solid lines in Fig. 2 are the expected resistivity obtained by numerically integrating Eq. (3) for top-surface specularity values of $p_1=0$, 0.5, 1, and using λ values of 39 and 333 nm for 298 and 77 K, respectively. The Cu–MgO interface is expected to yield completely diffuse ($p_2=0$) electron scattering since, based on our previous results,[4] $\rho$ for air-exposed Cu layers follows the FS prediction for completely diffuse scattering on both surfaces ($p_1+p_2=0$). All measured data points are below the $p_1=0$ line, indicating that the top surface exhibits partially specular scattering. The average $p_1$ value for all samples is $0.6\pm0.1$ at room temperature and $0.7\pm0.1$ at 77 K. The slightly lower value in liquid nitrogen is within the uncertainty of the room temperature value but may also indicate enhanced specular scattering due to flattening of the electrostatic surface potential associated with polarized physisorbed nitrogen on the Cu surface. The data also suggests a tendency toward lower $p_1$ values for increasing $d$, which may be attributed to the surface roughness, which is expected to increase with increasing $d$, leading to a decrease in the average width of atomically smooth terraces and, in turn, a decrease in specular surface scattering.

Figure 3 is a plot of the resistivity of two 27-nm-thick and one 39-nm-thick Cu(001) layers that were capped *in situ* with Ta overlayers of variable nominal thickness $t_{Ta}$. The resistivity increases with the addition of Ta, for example, from $2.26\pm0.05$ $\mu\Omega$ cm for a pristine Cu(001) surface to $2.59\pm0.07$ $\mu\Omega$ cm after deposition of 1–2 Ta monolayers ($t_{Ta}=0.3$ nm) onto a $d=27$ nm Cu layer. Further Ta deposition results in negligible (<2%) changes in $\rho$. The 39 nm sample shows a comparable but smaller resistivity increase from $2.28\pm0.05$ to $2.40\pm0.05$ $\mu\Omega$ cm. The smaller change is associated with the decreasing importance of surface scattering with increasing $d$. We attribute the change in $\rho$ with the addition of Ta to a transition from a partially specular to completely diffuse electron surface scattering. This is quantified by independently calculating $p_1$ values using Eq. (4) for all data points, as labeled in Fig. 3.

It is evident from the data in Fig. 3 that already the smallest amount of Ta deposited in these experiments corresponding to a nominal thickness of 0.3 nm results in an increase in $\rho$ that is consistent with a transition to completely diffuse scattering. In order to illustrate that, we have also plotted lines that represent the expected resistivity assuming an exponential decay of $p_1$ with increasing Ta thickness, using a constant decay length of 0.15 nm, corresponding to the interplanar spacing of bcc Ta along ⟨001⟩, which we also define as the nominal thickness of one Ta monolayer. Therefore, a single Ta monolayer is sufficient to cause diffuse surface scattering. This value (0.15 nm) represents an upper bound, since any decay length <0.15 nm would result in a steeper change in $\rho$ and would equally well describe the observed change in the measured resistivity.

In conclusion, *in situ* resistivity measurements on single crystal Cu(001) layers suggest that atomically smooth oxygen-free surfaces result in a flat periodic potential that causes conduction electrons that approach the Cu vacuum interface to specularly scatter back into the Cu layer. In contrast, the addition of Ta on the Cu surface causes a perturbation to the smooth interface potential, which effectively results in scattering centers that are displaced from the original Cu vacuum interface and cause destructive interference of the scattered electron wave and, in turn, a transition to completely diffuse surface scattering. The resistivity increase upon addition of Ta is particularly strong evidence for the initially specular scattering at Cu(001) surfaces and therefore resolves the longstanding question if specular surface scattering is possible for Cu.

This research has been supported by the NYSTAR Interconnect Focus Center at Rensselaer.

[1] http://public.itrs.net
[2] T. Kuan, C. Kinoki, G. Oerlein, K. Rose, Y.-P. Zhao, G. Wang, S. Rossnagel, and C. Cabral, Materials, Technology, and Reliability for Advanced Interconnects and Low-k Dielectrics, MRS Symposia Proceedings No. 612, D7.1.1. 2000 (unpublished).
[3] S. Rossnagel and T. Kuan, J. Vac. Sci. Technol. B **22**, 240 (2004).
[4] J. Purswani and D. Gall, Thin Solid Films **516**, 465 (2007).
[5] W. Steinhogl, G. Schindler, G. Steinlesberger, and M. Engelhardt, Phys. Rev. B **66**, 075414 (2002).
[6] W. Steinhogl, G. Schindler, G. Steinlesberger, M. Traving, and M. Engelhardt, J. Appl. Phys. **97**, 023706 (2005).
[7] K. Hinode, Y. Hanaoka, K. Takeda, and S. Kondo, Jpn. J. Appl. Phys., Part 2 **40**, L1097 (2001).
[8] H. Liu, Y. Zhao, G. Ramanath, S. Murarka, and G. Wang, Thin Solid Films **384**, 151 (2001).
[9] J. Plombon, E. Andideh, V. Dubin, and J. Maiz, Appl. Phys. Lett. **89**, 113124 (2006).
[10] Y. Ke, F. Zahid, V. Timoshevskii, K. Xia, D. Gall, and H. Guo, Phys. Rev. B **79**, 155406 (2009).
[11] E. H. Sondheimer, Adv. Phys. **1**, 1 (1952).
[12] E. Krastev, L. Voice, and R. Tobin, J. Appl. Phys. **79**, 6865 (1996).
[13] K. Yamada, W. Bailey, C. Fery, and S. Wang, IEEE Trans. Magn. **35**, 2979 (1999).
[14] T. Sun, B. Yao, A. P. Warren, V. Kumar, S. Roberts, K. Barmak, and K. R. Coffey, J. Vac. Sci. Technol. A **26**, 605 (2008).
[15] H. Hoffmann, J. Vancea, and U. Jacob, Thin Solid Films **129**, 181 (1985).
[16] V. Timoshevskii, Y. Ke, H. Guo, and D. Gall, J. Appl. Phys. **103**, 113705 (2008).
[17] B. Feldman, R. Deng, and S. Dunham, J. Appl. Phys. **103**, 113715 (2008).
[18] G. Kastle, H. Boyen, A. Schroder, A. Plettl, and P. Ziemann, Phys. Rev. B **70**, 165414 (2004).
[19] G. Kastle, A. Schroder, H. Boyen, A. Plettl, P. Ziemann, O. Mayer, J. Spatz, M. Moller, M. Buttner, and P. Oelhafen, Eur. J. Inorg. Chem. **2005**, 3691 (2005).
[20] J. Sambles, K. Elsom, and D. Jarvis, Solid State Commun. **32**, 997 (1979).
[21] J. Purswani and D. Gall, J. Appl. Phys. **104**, 044305 (2008).
[22] K. Fuchs, Proc. Cambridge Philos. Soc. **34**, 100 (1938).
[23] D. R. Lide, *CRC Handbook of Chemistry and Physics*, 84th ed. (CRC Press/Taylor and Francis, Boca Raton, FL, 2003).
[24] J. Lim, K. Mimura, and M. Isshiki, Appl. Surf. Sci. **217**, 95 (2003).
[25] J. Purswani, T. Spila, and D. Gall, Thin Solid Films **515**, 1166 (2006).

Downloaded 23 Jul 2009 to 128.113.37.139. Redistribution subject to AIP license or copyright; see http://apl.aip.org/apl/copyright.jsp